




# Implantable microchip containing oxygen-sensing paramagnetic crystals for long-term, repeated, and multisite *in vivo* oximetry

Maciej M. Kmiec<sup>1</sup> · Dan Tse<sup>1</sup> · Jesse M. Mast<sup>1</sup> · Rizwan Ahmad<sup>2</sup> · Periannan Kuppusamy<sup>1,3</sup> 

Published online: 8 July 2019

© Springer Science+Business Media, LLC, part of Springer Nature 2019

## Abstract

EPR oximetry is established as a viable method for measuring the tissue oxygen level (partial pressure of oxygen,  $pO_2$ ) in animal models; however, it has not yet been established for measurements in humans. EPR oximetry requires an oxygen-sensing paramagnetic probe (molecular or particulate) to be placed at the site/organ of measurement, which may pose logistical and safety concerns, including invasiveness of the probe-placement procedure as well as lack of temporal stability and sensitivity for long-term (repeated) measurements, and possible toxicity in the short- and long-term. In the past, we have developed an implantable oxygen-sensing probe, called OxyChip, which we have successfully established for oximetry in pre-clinical animal models (Hou et al. *Biomed. Microdevices* **20**, 29, 2018). Currently, OxyChip is being evaluated in a limited clinical trial in cancer patients. A major limitation of OxyChip is that it is a large ( $1.4\text{ mm}^3$ ) implant and hence not suitable for measuring oxygen heterogeneity that may be present in solid tumors, chronic wounds, etc. In this report, we describe the development of a substantially smaller version of OxyChip ( $0.07\text{ mm}^3$  or 70 cubic micron), called mChip, that can be placed in the tissue of interest using a 23G syringe-needle with minimal invasiveness. Using *in vitro* and *in vivo* models, we have shown that the microchip provides adequate EPR sensitivity, stability, and biocompatibility and thus enables robust, repeated, and simultaneous measurement from multiple implants providing mean and median  $pO_2$  values in the implanted region. The mChips will be particularly useful for those applications that require repeated measurements of mean/median  $pO_2$  in superficial tissues and malignancies.

**Keywords** EPR · Oximetry ·  $pO_2$  · Microchip · OxyChip · Multisite · Composite fitting · Tumor

## 1 Introduction

Tissue oxygen level (commonly expressed as *partial-pressure of oxygen*;  $pO_2$ ) is a critical determinant in several pathophysiological processes, including cardiovascular diseases, cancer, peripheral vascular diseases and wound healing (Kulkarni et al. 2007). Knowledge of tissue  $pO_2$  and its dynamics can help clinicians to make effective prognosis and treatment

decisions and can be used as a biomarker for monitoring treatment outcome. Therefore, it is desirable to have techniques capable of measuring tissue  $pO_2$  (oximetry), with sufficient sensitivity, accuracy, and reliability. Of the several promising techniques, oximetry based on electron paramagnetic resonance (EPR) has many advantages, including the ability to make *real-time*, *in vivo*, and repeated measurements of tissue  $pO_2$  (Ahmad and Kuppusamy 2010). In addition, EPR oximetry is unique in terms of its ability to make direct measurement of the absolute value of oxygen concentration ( $pO_2$ ).

EPR oximetry is currently established as a viable method for measuring tissue oxygen levels in several animal models of diseases (Ahmad and Kuppusamy 2010; Swartz et al. 2014a); however, the same has not yet been established for human measurements. A major reason, which limits the translation of the potential EPR oximetry for clinical use, is the requirement that an oxygen-sensing paramagnetic probe (molecular or particulate) needs to be placed at the site/organ of measurement. The placement of a foreign body/probe/device in the tissue may pose certain logistical and safety concerns on

✉ Periannan Kuppusamy  
kuppu@dartmouth.edu

<sup>1</sup> Department of Radiology, Geisel School of Medicine, Dartmouth College, 1 Medical Center Drive, Ruben 601, Lebanon, NH 03756, USA

<sup>2</sup> Department of Biomedical Engineering, The Ohio State University, Columbus, OH 43210, USA

<sup>3</sup> Department of Medicine, Geisel School of Medicine, Dartmouth College, 1 Medical Center Drive, Ruben 601, Lebanon, NH 03756, USA

the (i) invasiveness of the placement of the probe by infusion, injection or implantation, (ii) lack of temporal stability and sensitivity of the probe for long-term (repeated) measurements, and (iii) possible unknown toxicity profile of the probe in the short- and long-term. In spite of the innovative developments made in this field over the last 3 decades (Elas et al. 2006; Epel and Halpern 2015; Ilangovan et al. 2004a; Krishna et al. 2002; Kuppusamy et al. 1998; Matsumoto et al. 2006, 2018; Velan et al. 2000), translation of these technological research advancements to clinical use has been hampered by the above limitations.

Our laboratory has undertaken the first step to bring EPR oximetry to the clinical realm, with some significant compromises; the most important of them is to give up spatial resolution (imaging) of oxygen data (Ilangovan et al. 2004b; Khan et al. 2007; Meenakshisundaram et al. 2009a; Mohan et al. 2009; Swartz et al. 2014a, b). Currently, our focus is on establishing EPR oximetry for 'point' measurements of  $pO_2$ , repeatedly and noninvasively for the long term, without having to re-introduce the sensor. Toward this goal, we have developed an implantable oxygen-sensing probe, called OxyChip (Hou et al. 2017a, 2018; Meenakshisundaram et al. 2009a; Meenakshisundaram et al. 2009b), and with FDA/CDRH approval we have carried out initial safety/feasibility clinical measurements in the tumor of several cancer patients. The OxyChip, which is currently approved by FDA for clinical trial studies, is made in the form of a 0.6-mm  $\times$  5-mm cylindrical pellet consisting of 40% lithium octa-n-butoxynaphthalocyanine (LiNc-BuO) microcrystals embedded in 60% of polydimethylsiloxane (PDMS) polymer (Meenakshisundaram et al. 2009a). Although the chip requires one-time placement in the tissue by a minimally invasive procedure using an 18G syringe needle, the  $pO_2$  measurements can be carried out from the chip for weeks, months or longer, repeatedly and non-invasively (Hou et al. 2018).

While we have successfully developed and established the applicability of OxyChip for oximetry in deep tissues such as deep-seated tumors (Hou et al. 2017b; Khan et al. 2015; Mast and Kuppusamy 2018), the OxyChip has certain limitations for applications that may not require deep-tissue oximetry or that oxygen data from a single site in the tissue may not be an adequate representation of the entire tissue oxygenation. For example, superficial malignant tumors (recurrent, metastatic tumors or primary ones) located close to skin, hypodermis, or skin muscle tissues, topical wounds, diabetic foot ulcers, certain neuropathic pathologies, etc. may require a sensor that is small and uses a minimally invasive placement procedure, e.g., with a fine needle, and removal, if necessary. The current OxyChip, that has been developed for deep-tissue oximetry is too large (1.4 mm<sup>3</sup>) for superficial tissue applications. The

large size of the probe may also limit the number of sensors that can be implanted in the tissue/area of interest, causing technical challenges to get reliable and useful oxygen measurements from multiple implants in close proximity to each other. This is a major limitation that may underestimate its usefulness for those tissues such as tumor and wound where oxygen heterogeneity is a significant problem to be addressed.

To overcome these limitations, we have developed a new version of oxygen-sensor, called mChip, which is small enough (0.3-mm diameter  $\times$  1-mm length) for multiple implantations in a single site with minimal invasiveness, but capable of providing adequate EPR sensitivity and oxygen at depths of 1–4 mm. In this first report, we present the results of fabrication, characterization, validation, and establishment of the mChip for possible clinical applications. The results suggest that the mChips are stable and sensitive enabling robust measurements of mean and median values of oxygen concentration in tissues. The mChips will be particularly useful for those applications that require repeated and reliable measurements of  $pO_2$  in superficial tissues and malignancies.

## 2 Materials and methods

### 2.1 Fabrication of mChip

The mChips are made of paramagnetic, oxygen-sensing LiNc-BuO microcrystals embedded in polydimethylsiloxane (PDMS) polymer. LiNc-BuO crystals were prepared as reported (Pandian et al. 2003). PDMS was obtained in two parts, as medical grade silicone elastomer (MED 4210) and cross-linker (A-103-C) from factor II (Lakeside AZ). Fabrication of mChips by embedding of LiNc-BuO crystals in PDMS was done as reported (Meenakshisundaram et al. 2009a) with the following modifications. Needle-shaped microcrystals of LiNc-BuO (of size 10–60  $\mu$ m) were sonicated in water (Pandian et al. 2003) and vacuum-dried at room temperature to obtain fine powder with particle size  $\leq 1$   $\mu$ m, as verified by a particle size analyzer. After mixing 10:1 ratio of PDMS elastomer and cross-linker on a weighing boat, sonicated LiNc-BuO powder was added to the PDMS mixture (40% w/w) followed by approximately 2% platinum accelerator. The mixture as thoroughly mixed using a glass rod and quickly force-drawn into several 23G light-wall PTFE tubes (Part# STT-26-C, Component Supply Co) by a pressure differential to about 5-cm length. The tubes were then kept in an oven at 80 °C for 12 h for curing. The cured product was extruded from the tubes by gentle pulling and cut into 1-mm-long pieces of mChip under microscope. The mChips were taken in a beaker containing water and stirred with a magnetic pellet continuously for 72 h to remove any sticking or loose particulates on the surface, dried, and steam-sterilized in the autoclave at 121 °C using gravity cycle of 40 PSI for 30 min.

## 2.2 EPR measurements

EPR measurements were performed to characterize the functioning of mChips including the effect of oxygen, temperature, stability after treatments, optimal instrument measurement parameters, and tissue oximetry using home-built CW L-band EPR spectrometer, as described previously (Hou et al. 2018). Some experiments including mechanical stress and solvent extraction measurements were performed using EMX EPR spectrometer (ER041X by Bruker BioSpin Corporation) operating at X-band frequency and equipped with the ER 4119HS high-Q cavity. Unless mentioned, all EPR measurements were made under non-saturation conditions of RF power and modulation amplitude.

## 2.3 Functional characterization of mChips

A set of 5 mChips was used for each of the following tests: autoclave sterilization, ultrasound sonication, exposure to ionizing radiation, mechanical stress and solvent extraction studies. After each test, the mChips were measured individually using X- or L-band EPR spectrometry as above. EPR signal intensity (AUC), amplitude (peak-to-peak), linewidth (HWFMM) and oxygen sensitivity (G/mmHg) measured under different oxygen exposure levels ( $pO_2$ : 0–228 mmHg) were used as metrics of mChip functionality.

## 2.4 Oxygen sensitivity calibration of mChips

Calibration of oxygen sensitivity of mChips was done using gases (Airgas) with known oxygen concentration between 0 mmHg (0%) to ~160 mmHg (21%). At least 5 different oxygen concentrations were used. The measured linewidths (HWFMM; G) were plotted against  $pO_2$  (mmHg) and fitted with a linear function to obtain oxygen sensitivity (G/mmHg) and anoxic linewidth (G). Unless mentioned otherwise, all calibrations were made at room temperature and ambient pressures (Hou et al. 2018).

## 2.5 Sterilization, irradiation and other treatments

Sterilization of mChips was done by autoclaving at 121 °C using gravity cycle (gravity30/dry30 40 PSI) in a gravity steam sterilizer (Gettinge Group; Model 522-CS). Irradiation was performed by exposing mChips to Cesium-137 source (emitting gamma rays with 661 keV energy (Irradiator - Shepherd & Associates, USA). The sonication procedure was done using 37-kHz frequency for 20 min at room temperature using Elmasonic P-30-H sonicator at 1/3 of its maximum power in sweep mode. For testing mechanical stress and residue/loose particulates on the surface, 5 mChips were taken in a small beaker containing distilled water and second group of 5 into a beaker with ethanol. The mChips in a solution were

magnetically stirred at 50 °C temperature for 3 sequential sessions of 72 h each session and tested. At the end of each session, the extracts were tested in 50- $\mu$ l capillary tubes using X-band EPR spectrometer equipped with ER 4119HS high-Q cavity, oriented horizontally to avoid settling of any particulates at the bottom of the capillary.

## 2.6 Cell viability assay

Rat skeletal muscle myoblast cells (L6; from ATCC) were plated in 6-cm dishes and incubated without or with 5 mChips/dish in culture medium for 48 h. Cells were collected after 48 h of incubation and stained with Live/Dead Flexible Violet Dead Cell Stain Kit (Life Technologies, Grand Island, NY) and analyzed by flow cytometry.

## 2.7 RF depth sensitivity testing

The mChip is designed for superficial tissue implantations, and hence it is important to establish maximum depth sensitivity or maximum depth at which the mChip can be detected. The depth sensitivity is dependent on various factors including resonance frequency (in this case L-band), modulation amplitude, RF power and resonator used for the measurement. We used an artificial tissue emulating (ATE) phantom consisting of ethylene glycol (laboratory grade) and gelatin (reagent grade) from Carolina Biological Supply Company (Whitsett, NC, USA). To determine the intrinsic electromagnetic properties of the tissue and ATE phantom Agilent Technologies E5071C ENA Series Network Analyzer with Keysight 85070E Dielectric Probe Kit designed for measuring liquids and conformable solids were used. Phantom made of 20% w/v of gelatin in ethylene glycol had close dielectric properties to the human muscle tissue. To extend the scope of this test and take into account the distribution of the B1 field generated by the surface loop resonator inside ATE phantom finite element simulations were performed. ANSYS HFSS v18 application was used to simulate resonator and ATE phantom geometry and visualize the B1 field inside the ATE phantom. Inside small semi-solid ATE phantom mChip was placed at different distance (depth) from the surface loop resonator and surface of the phantom. The mChip was placed in a flexible polyethylene tubing (1-mm OD; 0.6-mm ID) to provide the flow of gasses with different oxygen concentrations.

## 2.8 *In vivo* EPR measurements

Muscle  $pO_2$  measurements in mice were performed using an L-band (1.2 GHz) spectrometer equipped with a surface-loop resonator (Salikhov et al. 2003). Animals (mice) were placed on a plastic bed plate such that the location of mChip implantation in the muscle was just beneath the loop, and approximately centered at the active volume of the loop resonator.

Body temperature, during measurements, was monitored using a thermistor rectal probe, and maintained at  $37 \pm 1$  °C using a thermostatically controlled, heated pad and a flow of warm air. Post-implantation  $pO_2$  measurements in muscle were made for up to 8 weeks.  $pO_2$  measurements were made continuously during mice breathing room-air or gas mixtures containing 10% or 95% oxygen. Typically, baseline measurements of  $pO_2$  were made during the first 10–20 min, which was followed by nose-cone breathing of higher or lower oxygen content for up to 20 min. Subsequently, the breathing gas was switched to room air, and EPR measurements were continued for another 10–20 min. Unless mentioned, all EPR spectra were measured under non-saturation RF power and modulation amplitude.

### 2.8.1 Animal preparation

All the animal procedures were approved by the Institutional Animal Care and Use Committee of Dartmouth College. Twelve adult female Balb/c mice (20–30 g; Charles River Laboratories, MA) were used for muscle tissue experiments and two male NOD-scid-gamma (NSG) mice (bred at Dartmouth Animal Resource Center) were used for tumor measurements. The animals were separately maintained in a clean 12 h light-dark cycle with free access to food and water. For all surgical procedures, 2.5–3.0% isoflurane in 30%  $O_2$  was used for anesthesia induction, and 1.5–2% isoflurane for anesthesia maintenance.

### 2.8.2 Implantation of mChip in the skeletal muscle

The effect of long-term implantation in the muscle tissue of mouse was determined. Before implantation, mChips were calibrated and then sterilized by autoclaving at 121 °C for 30 min. The mice were anesthetized using 2–2.5% of isoflurane in 30% oxygen administered via nose-cone breathing. The right hind leg was shaved, and the skin was prepared with a betadine and 70% alcohol scrub. Ten mice were implanted with a single mChip and two mice were implanted with 4 mChips. The chips were implanted in the biceps femoris of right limb of mice with a 23G needle at a depth of 2–4 mm from the surface of the skin.

### 2.8.3 Measurement of $pO_2$ in the muscle

Measurements of skeletal muscle  $pO_2$  were carried out in 12 mice once a week for 8 weeks. During each session, baseline  $pO_2$  values were first measured for 30 min. To mimic hypoxic or hyperoxic conditions,

the animals were breathing 10% or 100% oxygen for 5–10 min via nose cone. At the end of the study, tissues surrounding the mChip were removed and stored at 10% formalin for histological and H&E analyses.

## 2.9 Tumor growth, mChip implantation and $pO_2$ measurements

NOD-scid-gamma (NSG) mice (bred at Dartmouth Animal Resource Center) were injected with  $5 \times 10^6$  AsPC-1 tumor cells in the flank. When the tumors were palpable, 14 days post-injection, 2–4 mChips were implanted into the tumor at depths of 2–4 mm. Repeated  $pO_2$  measurements were carried out as described above.

## 2.10 Statistical analysis

A paired t-test was used to compare the  $pO_2$  values at different time points within the same group. The paired comparison reduces the effects of animal-to-animal heterogeneity and eliminates differences in the baseline  $pO_2$ . The comparisons of linewidth and signal intensity between mChips were made using a Student's t-test for unpaired samples. All data were expressed as Mean  $\pm$  SE. A *P* value  $< 0.05$  was considered statistically significant.

## 3 Results

### 3.1 EPR sensitivity

The mChips were fabricated in the shape of a cylindrical fiber with 0.3-mm diameter and 1-mm length. The shape and size of the mChips were chosen to be able to insert them in the tip of a 23G syringe-needle for implantation in tissues (Fig. 1a). The EPR sensitivity of the mChips was measured under three different oxygen environments with  $pO_2$  values 0, 15.2, 38 mmHg and compared to OxyChip, which is currently used as single implant in cancer patients. The EPR signal intensity (AUC) of a single mChip was approximately 1/20th of that of OxyChip, irrespective of the oxygen content in the equilibrating gas mixture (Fig. 1b). On the other hand, the intensity of 20 mChips kept within the surface-loop resonator, which is known to have a nonuniform B1 field (He et al. 2002), was about 17% lower compared to single OxyChip, suggesting that the spread of the mChips (mimicking distribution of multiple chips in the tissue) did not compromise the detection sensitivity. The results demonstrated that the EPR sensitivity of the

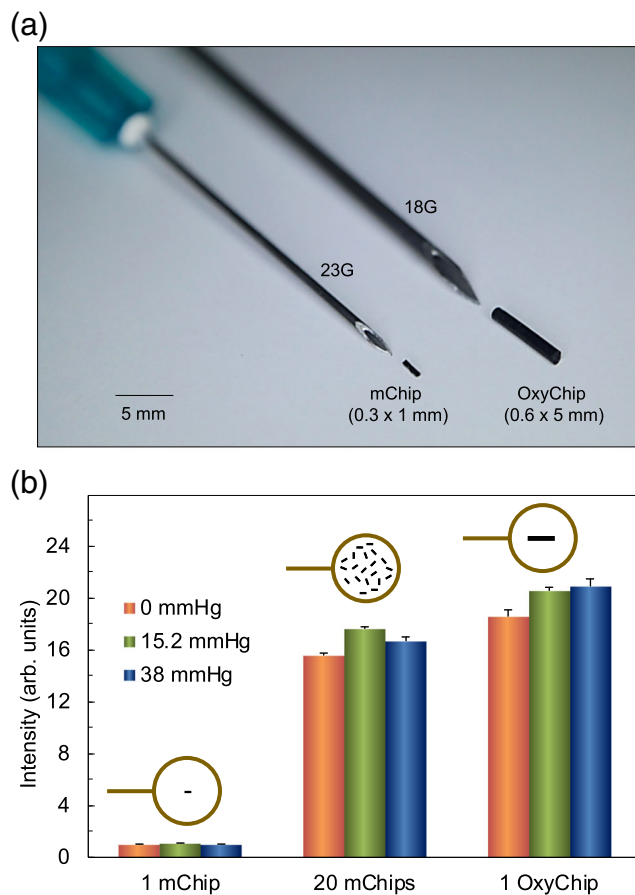


**Fig. 1** Comparison of mChip to OxyChip. **a** Visual comparison of the sizes of mChip and OxyChip with needles used for implantation in living tissues. **b** Comparison of the signal intensities (double integral, AUC) from 1 mChip, 20 mChips and 1 OxyChip measured at L-band using the same instrumental settings but under different pO<sub>2</sub> values 0, 15.2 and 38.0 mmHg. The illustrations show the approximate placement of the chip(s) within the surface-loop resonator. Data represent Mean  $\pm$  SE ( $N = 5$ ). The results show that the EPR sensitivity of mChips is approximately 1/20th of OxyChip

mChips is not compromised, from what is expected based on its size and spin content, up on miniaturization.

### 3.2 Oxygen sensitivity

The mChips exhibited a single narrow EPR spectrum with a line-width of about 0.1 G (HWHM) under anoxic conditions. Exposure of the chips to molecular oxygen induced a reversible pO<sub>2</sub>-dependent broadening of the EPR spectrum (Fig. 2a). The line-width of the spectrum exhibited a linear relationship to pO<sub>2</sub> in the range 0–760 mmHg (100% O<sub>2</sub>). The oxygen-response of the mChip was comparable to that of OxyChip, although the OxyChip showed a slightly higher sensitivity in comparison to mChip, (0.0117 vs 0.0105 G/mmHg (Fig. 2c), possibly attributed to their sizes and magnetic field

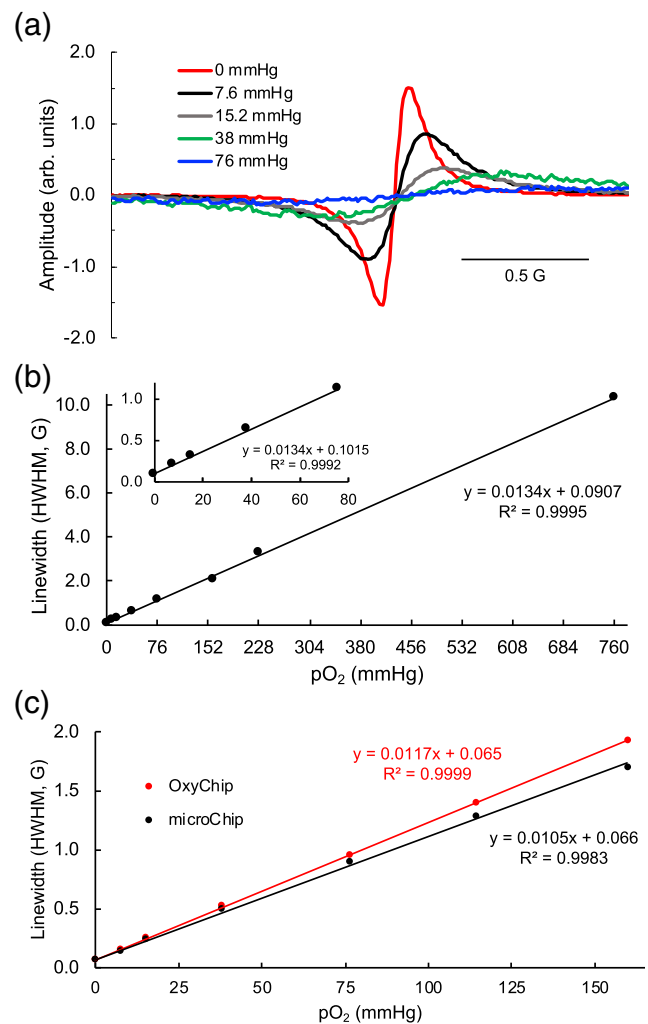


**Fig. 2** Effect of molecular oxygen on the EPR spectrum of mChip. EPR spectra of mChip were obtained under equilibrium with the following pO<sub>2</sub> values (in mmHg): 0 (0% O<sub>2</sub>); 7.6 (1% O<sub>2</sub>); 15.2 (2% O<sub>2</sub>); 38 (5% O<sub>2</sub>); 76 (10% O<sub>2</sub>) under atmospheric pressure. **a** Representative scans made at room temperature (21.7 °C) at each pO<sub>2</sub> as indicated. The spectra show oxygen-dependent line-broadening. **b** EPR linewidths of mChip were determined in the pO<sub>2</sub> range 0–760 mmHg (100% O<sub>2</sub>) at room temperature (21.7 °C). A linear dependence between linewidth and pO<sub>2</sub> is seen for up to 100% oxygen. The inset shows the linearity of calibration in the pO<sub>2</sub> range 0–76 mmHg (10% O<sub>2</sub>). **c** Comparison of the calibration curves for mChip and OxyChip in the pO<sub>2</sub> range 0–160 mmHg (21% O<sub>2</sub>). While both curves show a linear variation of line-width with pO<sub>2</sub>, the OxyChip shows a slightly higher sensitivity to oxygen, that is 0.0117 vs 0.0105 G/mmHg

homogeneity. The results established a linear calibration and comparable oxygen sensitivity to OxyChip.

### 3.3 Effect of temperature and time response of oxygen sensitivity

The oxygen sensitivity of the mChip was dependent on temperature, as shown at 21.7 °C (room temperature)

and 37 °C (physiological temperature) in Fig. 3a. It should be noted that the anoxic linewidth was not affected by temperature in the range studied. The time responses of the chip toward oxygenation and deoxygenation were determined by rapidly switching the oxygen content (pO<sub>2</sub>) in equilibrating gas mixture from 0 mmHg to 7.6, 15.2, 38, or 76 mmHg, and back to 0 mmHg, as described previously (Kmiec et al. 2019). EPR spectra were acquired continuously during baseline, oxygenation and deoxygenation periods to determine the time course of pO<sub>2</sub> sensed by the chip. The results (Fig. 3b) demonstrated a rapid response of mChip, in about a few seconds, to changing oxygen concentration suggesting that the mChip can respond to dynamic changes in oxygen concentration in the order of seconds.

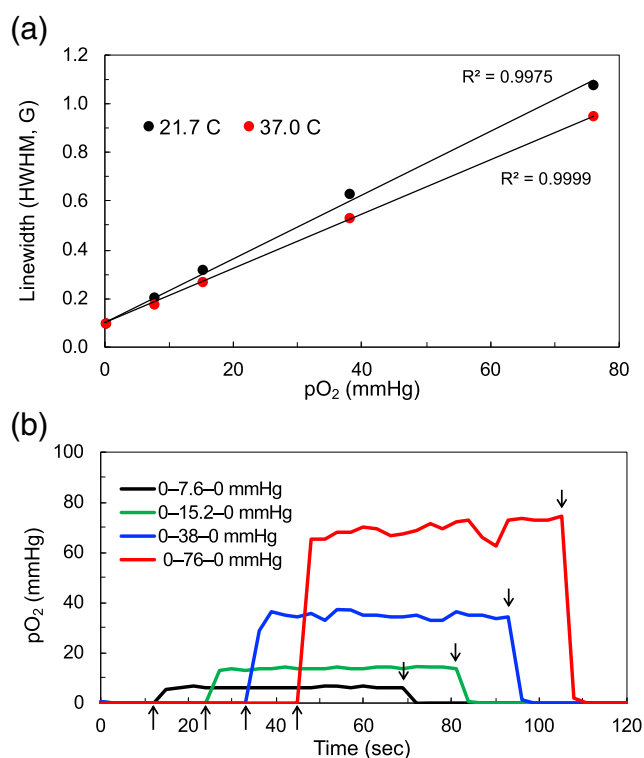


**Fig. 3** Effect of temperature and time-response of mChip to oxygen. **a** Dependence of EPR spectral linewidth (HWHM) on pO<sub>2</sub> in the equilibrating gas mixture was measured at room (21.7 °C) and physiological (37 °C) temperatures. A linear dependence between linewidth and pO<sub>2</sub> is seen at each temperature. The oxygen sensitivity is temperature dependent (0.0131 G/mmHg at 21.7 °C vs 0.0112 G/mmHg at 37 °C), while the linewidth at pO<sub>2</sub> = 0 is unchanged (0.101 G). **b** Time response of mChip to dynamic changes in equilibrating pO<sub>2</sub>. The chips initially kept at equilibrium with pO<sub>2</sub> = 0 mmHg were quickly exposed to higher pO<sub>2</sub> values (7.6–76 mmHg) for 60 s and switched back to 0 mmHg. The arrows indicate the times at which the gases were switched. The results show that the mChips respond almost instantly and reach equilibrium to the new level in seconds

### 3.4 Stability under adverse conditions

We next determined the stability of mChips under conditions of adverse treatment conditions that are encountered in their use for biological, including clinical, applications. The treatment conditions we studied were sterilization by autoclave, sonication by ultrasound, and exposure to ionizing radiation. EPR measurements of linewidth were carried out on mChips before and after treatment. Figure 4a shows the effect of treatment on linewidth measured under different pO<sub>2</sub> values, from 0 to 228 mmHg. Figure 4b shows the effect of treatment on the oxygen sensitivity (calibration) for the treatment groups. The results showed that there was no significant change in both the linewidth and oxygen sensitivity of mChips subjected to autoclave, sonication or irradiation. Exposure to radiation, even at a very high dose (300 Gy) did not affect EPR and oxygen sensitivity of the chips. We further determined the effect of radiation dose rates, namely 1 Gy/min and 10 Gy/min, for a total of 60-Gy delivery on the mChips. Samples exposed to the high-energy radiation may take cool-down time to reach stability and exhibit exposure-induced changes in their property. We exposed the chips to 60-Gy radiation and made the oxygen-sensitivity measurement at different times (3 min, 10 min and 3 h) after exposure. The results, also shown in Fig. 4b, suggested that the exposure rate or the time after exposure had no significant effect on the oxygen sensitivity of the chips. Taken together, the data suggested that the mChips are robust and stable against adverse exposure conditions.

### 3.5 Stability against solvent extraction

To evaluate the stability of mChips against long-term and extreme conditions of solvent extraction, we incubated the mChips with continuous stirring (using a magnetic pellet stirrer) in water or ethanol at 50 °C for 9 days, with 3 consecutive sessions of 3 days/session. At the end of each 3-day session, the extraction media were measured using X-band EPR spectroscopy to determine the presence of any debris (LiNc-BuO particulates) leached into the medium. Figure 5 shows representative EPR spectra of the chip (before and after 9 days of solvent extraction) and media from incubation in water at 50 °C for 3–9 days. In both water and ethanol incubations, the extracts did not show any EPR signal suggesting that there were no EPR-detectable residues of the chip (fragments of LiNc-BuO crystals). Overall, the results indicated that there were no detectable residues of the LiNc-BuO particulates during the 3–9 days of incubation with continuous stirring in water or ethanol.

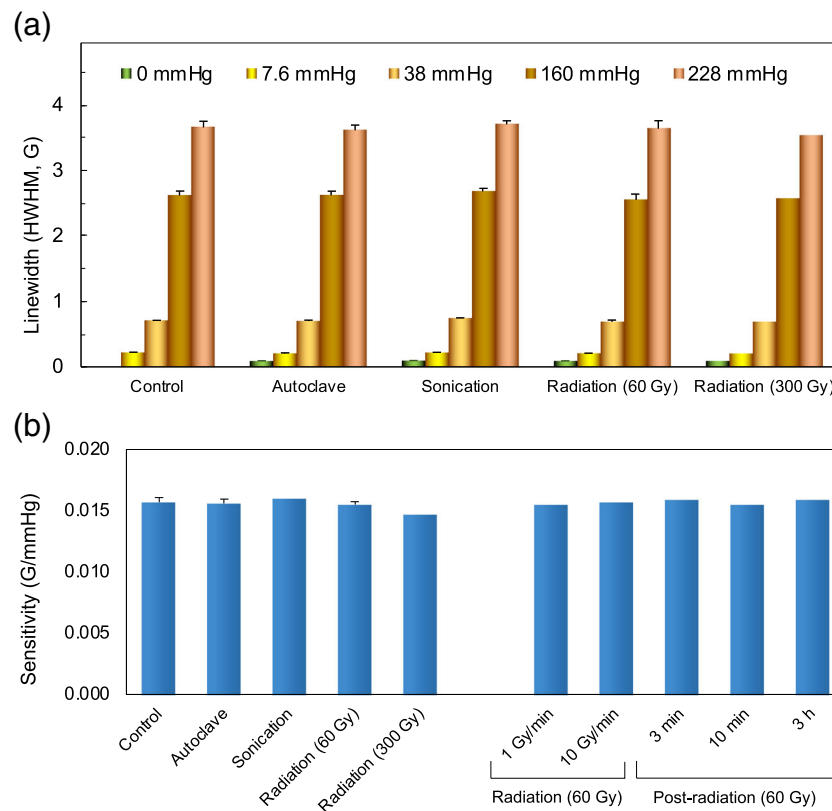


**Fig. 4** Effect of sterilization and radiation on the EPR oxygen sensitivity of mChip. The effects of sterilization by autoclave, exposure to ionizing radiation (60 and 300 Gy) and sonication by ultrasound on oxygen sensitivity of mChip were determined using EPR. After treatment or exposure, EPR spectra of mChips were obtained under equilibration with gas mixtures containing oxygen and nitrogen with the following pO<sub>2</sub> (in mmHg): 0 (0% O<sub>2</sub>); 7.6 (1% O<sub>2</sub>); 38 (5% O<sub>2</sub>); 160 (21%); 228 (30% O<sub>2</sub>) under atmospheric pressure. **a** Effect of treatment on linewidth

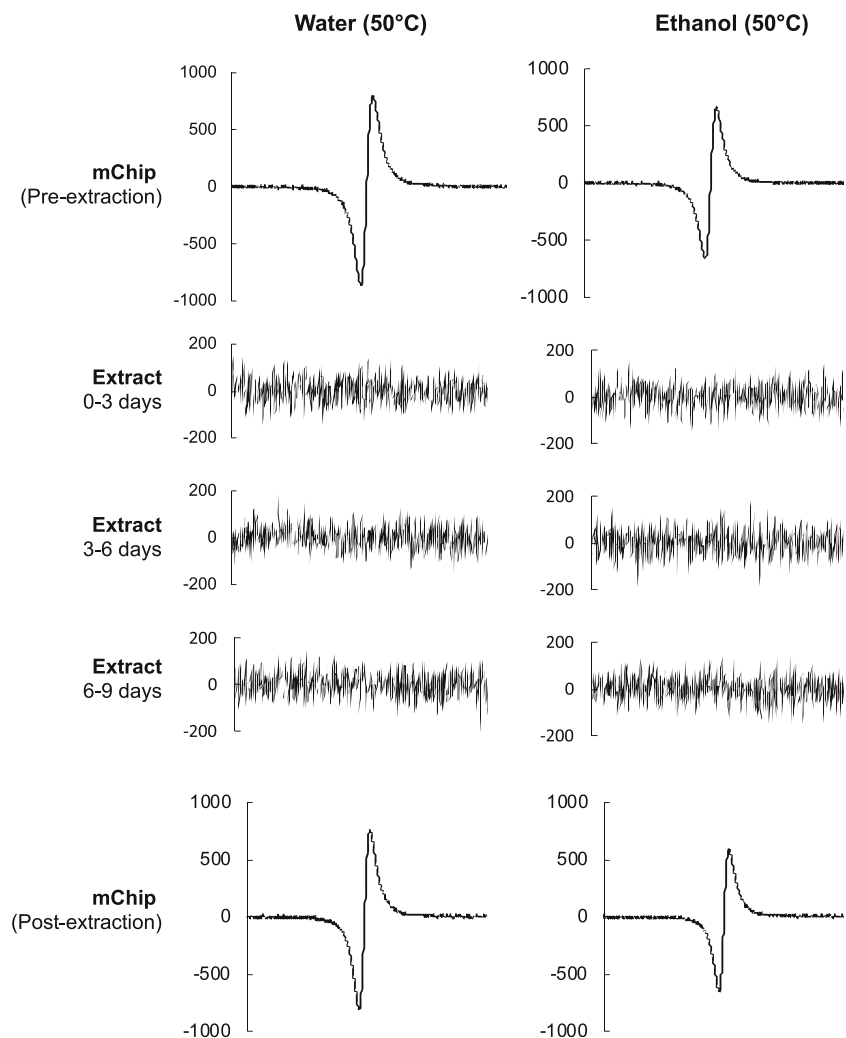
(Mean  $\pm$  SE; N = 5 mChips) at each pO<sub>2</sub> value. There are no significant differences between the untreated (Control) and treated groups. **b** Oxygen sensitivity (G/mmHg) for each treatment. Also shown are the values for 60-Gy radiation delivered at 1 or 10 Gy/min and measurements made 3 min, 10 min or 3 h after delivery of 60 Gy radiation. Data represent Mean  $\pm$  SE; N = 5 mChips or single measurement. The results show that the oxygen sensitivity of mChips is not affected by sterilization procedures or exposure to high-energy radiation

### 3.6 Effect of RF (microwave) power and modulation amplitude on EPR sensitivity and linewidth of mChip

In continuous wave (CW) EPR oximetry, the magnitude of incident microwave power needs to be optimized for maximum SNR and distortion-free linewidth measurements. While EPR signal amplitude varies directly with RF power, the short T<sub>1</sub>/T<sub>2</sub> of mChips may get easily saturated leading to signal broadening and reduction of the signal intensity. We determined the effect of RF power, from -11.1 dBm (0.078 mW) to 18.4 dBm (70 mW), on signal amplitude and linewidth, under different oxygen concentrations. As shown in Fig. 6a, the RF power has a profound saturation effect on mChips at low oxygen concentrations (pO<sub>2</sub>: 0–15.2 mmHg) while the effect is negligible at pO<sub>2</sub> values >15.2 mmHg. A similar effect, namely RF power-induced increase in linewidth, is observed at pO<sub>2</sub> values

15.2 mmHg or less (Fig. 6b). For example, when EPR linewidth is less than 0.2 G distortion (broadening) occurs at 12.3 dBm (~17 mW). In case of anoxic linewidth (<0.1 G), the line-width increases at 3.4 dBm (~2.2 mW). The results suggest that optimal signal (SNR) with distortion-free signal from mChip requires a careful consideration of RF power level. Another critical factor that needs to be optimized for mChip is the strength of magnetic field modulation used in CW EPR oximetry. As with RF power, field modulation increases SNR; however, beyond certain threshold it will result in artificial increase of linewidth and saturation of signal amplitude. We determined the effect of modulation amplitude, from 1/10th to 10-fold of true linewidth, under different oxygen concentrations. As shown in Fig. 6c–d, the modulation amplitude causes saturation effect on the amplitude and observed linewidth of mChips when the magnitude of modulation amplitude exceeds one-half of the true linewidth at each oxygen concentration.

**Fig. 5** Effect of solvent extraction on mChip. mChips were incubated with continuous stirring in water or ethanol at 50 °C for a total 9 days with 3 consecutive sessions of 3 days/session. At the end of each 3-day session, the extraction media were measured using X-band EPR spectroscopy to determine the presence of any debris (LiNc-BuO particulates) leached into the medium. Shown are representative EPR spectra of the chip before and after extraction and that of the extracts collected at the end of each 3-day session, for water and ethanol solvent. Of note, the chip spectra were measured as single scans, while the spectra of the extracts represent sum of 100 scans, while all other data acquisition parameters were unchanged. The results indicate that there are no EPR detectable residues of the chip following 3–9 days of incubation with continuous stirring in water or ethanol at 50 °C



### 3.7 RF penetration depth on EPR sensitivity of mChip

EPR sensitivity of the implant as a function of depth in tissue is mostly dependent on the frequency, distribution of the B1 field generated by the resonator, amount of paramagnetic material (size of the sensor) and type of the sample (dielectric losses, conductivity) where the implanted oxygen sensor is located. Depending on the resonance frequency, typical surface loop resonator has limited depth of penetration in living tissue (Pollock et al. 2010). To evaluate the EPR detection sensitivity of mChips as a function of implantation depth in tissues, simulations were performed to visualize B1 field distribution (Fig. 7a). The simulation results were validated using EPR measurements on artificial tissue emulation ATE phantom (Mobashsher and Abbosh 2015). Parallel to the central cross-section of the phantom, a mChip in polyethylene tube was

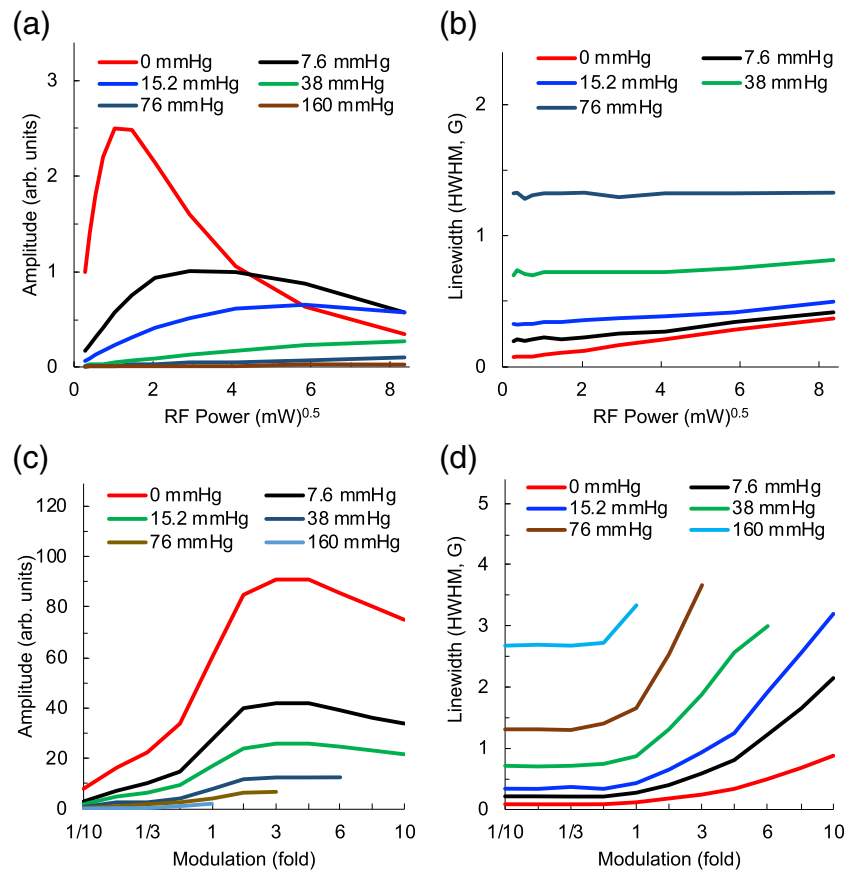
inserted at different depth 0–5 mm. Measurements were made at two power levels, namely  $-1.5$  dBm (0.7 mW) and 10.4 dBm (10.9 mW) under 7.6-mmHg oxygen environment. As seen in Fig. 7b, the SNR was strongly dependent on the power and depth of placement of the chip in the tissue. The results suggested that mChips can be measured in tissues up to 5-mm depth using L-band RF frequency.

### 3.8 Composite oximetry using multiple mChips

A major motivation for the development of mChip is the possibility of obtaining average (mean and median)  $pO_2$  in a region of interest using a single EPR scan of randomly implanted multiple mChips (Ahmad et al. 2008). To demonstrate the feasibility of such measurements, we used a phantom containing 4 mChips, each taken in a



**Fig. 6** Effect of RF power and modulation amplitude on EPR sensitivity and line-width of mChip. The effects of RF power and modulation field on EPR signal amplitude and linewidth were determined by measuring EPR spectra of mChip as a function of RF power under  $pO_2$  (in mmHg): 0 (0%  $O_2$ ); 7.6 (1%  $O_2$ ); 38 (5%  $O_2$ ); 160 (21%) at ambient conditions. **a, b** Variation of EPR signal amplitude and linewidth on RF power. **c, d** Variation of EPR signal amplitude and linewidth on modulation field, expressed relative (fold) to respective ‘undistorted’ linewidths. The results show that both RF power and modulation amplitude induce oxygen-dependent saturation of the signal amplitude and line-broadening



separate capillary tube connected to polyethylene tubing such that they can be equilibrated independently with a gas mixture of different  $pO_2$  (Fig. 8a). The 4-chip phantom with each chip equilibrated with 0, 7.6, 15.2 or 38 mmHg  $pO_2$  was placed under a surface-loop resonator and subjected to a magnetic field gradient of 6.5 G/cm across the tubes to resolve their EPR spectrum for qualitative identification of spectral components. Figure 8a shows the arrangement of the 4 chips and spectrum obtained without and with magnetic field gradient. It is seen that the 4 chips have been resolved well with signal amplitude and line-width corresponding to their respective  $pO_2$  exposure under magnetic field gradient. Under these conditions, a single-Lorentzian fit to the composite spectrum (without gradient) showed a  $pO_2$  of 5.8 mmHg, which was clearly different from the input mean  $pO_2$  of 15.2 mmHg (Fig. 8b). On the other hand, using a modified composite fitting algorithm, based on (Ahmad et al. 2008), to the same spectrum produced a mean and median value of 15.3 and 19.3 mmHg, respectively. The results agreed closely to the input data suggesting that multiple implants of mChips can be measured with a single scan

and without use of field gradients, and the mean/median  $pO_2$  values can be obtained from the composite spectrum.

### 3.9 Repeated *in vivo* measurement of muscle $pO_2$ using a single mChip

We next determined the feasibility of using mChip for repeated measurements of tissue oxygenation under *in vivo* conditions. We implanted single mChips in the biceps femoris of right limb of mice at a depth of 1–4 mm from the skin. The  $pO_2$  measurements were repeatedly made every week for 8 weeks in the healthy muscle (control group) and muscle exposed to a total 36-Gy radiation, delivered in  $2 \times 6$  Gy per week for the first 3 weeks. Representative EPR spectra obtained from control and irradiated muscle on week 4 are shown in Fig. 9a–b. Changes in muscle  $pO_2$  during the 8-week period are shown in Fig. 9c. Average values of muscle  $pO_2$  obtained from the respective groups in the first 3 weeks during irradiation (Pre-Radiation) and later 5 weeks (Post-Radiation) are shown in Fig. 9d. The results demonstrated the feasibility of using a single mChip for making repeated *in vivo* measurements of tissue oxygen over a period of 8 weeks.

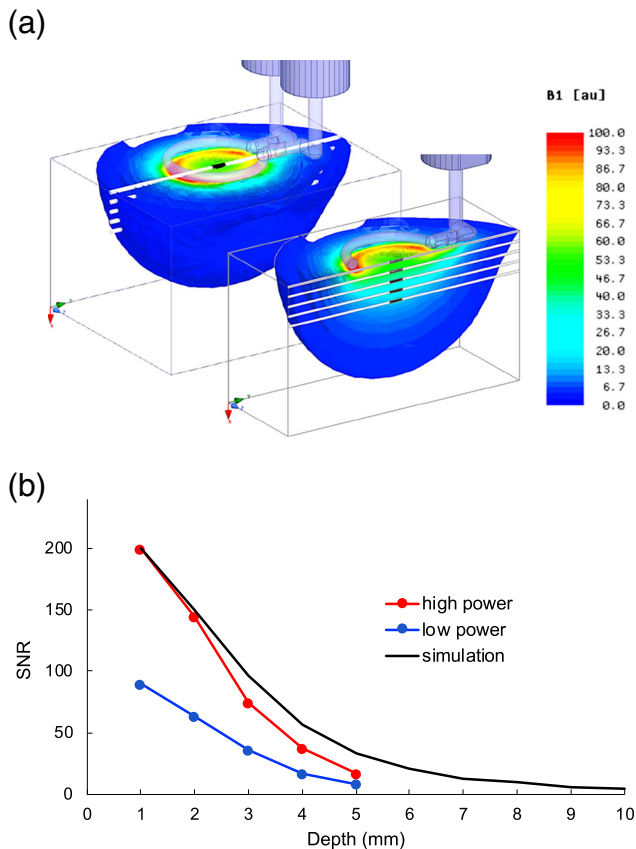


**Fig. 7** Effect of RF penetration depth on EPR sensitivity of mChip. The effect of RF penetration depth on mChip was determined using a tissue phantom. **a** Distribution of the B1 field generated by the surface-loop resonator and positions of the single mChip under the loop during the depth-sensitivity testing in a tissue-emulating material. **b** Simulated and measured SNR as a function of depth. The SNR measurements correspond to two power levels,  $-1.5$  dBm ( $0.7$  mW) and  $10.4$  dBm ( $10.9$  mW) at  $7.6$  mmHg oxygenation. The simulation results were normalized to high-power experimental results. The results show that mChip can be measured for up to 5-mm depth in tissues

### 3.10 Repeated *in vivo* measurements of changes in muscle $pO_2$ using multiple mChips

The utility of mChip for making repeated *in vivo* measurements of mean  $pO_2$  using multiple chips was demonstrated in a mouse model. We first tested for any cytotoxicity induced by the placement of multiple chips in tissues using an *in vitro* model of skeletal muscle cells (L6). Cells exposed to mChips for 48 h did not show any significant toxicity (Fig. 10a). Random implants of 4 mChips at depths of 1–4 mm from the skin were made in biceps femoris of right limb of mice. Repeated measurements of  $pO_2$  values were made every week for 8 weeks. Ultrasound images of the implanted region

revealed the presence of 4 mChips in the muscle (Fig. 10b). Changes in the mean muscle  $pO_2$  measured in two representative mice over a period of 8 weeks showed average  $pO_2$  values of  $14.2 \pm 1.5$  mmHg and  $10.4 \pm 1.4$  mmHg (Fig. 10c–d). We further determined the ability of mChip to respond to changes in tissue oxygenation. The mean  $pO_2$  values were calculated from the composite spectra obtained during mice breathing 30% oxygen and during 20 min of breathing carbogen gas (95%  $O_2$  + 5%  $CO_2$ ). Breathing carbogen gas showed a significant increase in the mean muscle tissue oxygenation (Fig. 10e). Similarly, mice breathing 10%  $O_2$  showed a significant drop in muscle  $pO_2$  and a partial recovery in 20 min following 30%  $O_2$  breathing (Fig. 10e). H&E staining of muscle tissue implanted with mChip recovered at 8 weeks showed no clear indication of any foreign body inflammatory response (Fig. 10f). No leakages of LiNbO<sub>3</sub> crystals from the chips were found in the track and surrounded muscle. The results established the ability of mChip for providing repeated *in vivo* measurements of mean  $pO_2$  using multiple chips.

### 3.11 Repeated *in vivo* measurement of changes in tumor $pO_2$ using multiple mChips

To establish the utility of mChips for repeated *in vivo* measurements of mean and median  $pO_2$  value in tumors, we made 4 implants of mChips in a human pancreatic cancer (AsPC-1) xenograft in mice.  $pO_2$  measurements were made repeatedly during tumor growth. Representative composite EPR spectra obtained from a single tumor on day 4, 7 and 14 after implantation of the chips are shown in Fig. 11a–c. Mean and median representation of  $pO_2$  values obtained from the composite data on days 4, 7 and 11 showed a progressive decrease in  $pO_2$  as a function of tumor growth (Fig. 11d). The results established the ability of mChip for making repeated *in vivo* measurements of mean and median  $pO_2$  in tumors using multiple chips.

## 4 Discussion

The present study establishes a new implantable oxygen-sensing probe, called mChip, for *in vivo* EPR oximetry with potential for clinical applications. The chip has a much smaller size (about 1/20th) compared to OxyChip (Hou et al. 2018), which is currently being evaluated in a clinical trial for deep tissue oximetry. The size of mChip is particularly suitable for implantation using a minimally invasive procedure and providing simultaneous measurement of oxygen concentration ( $pO_2$ ) from multiple implants to obtain oxygen distribution

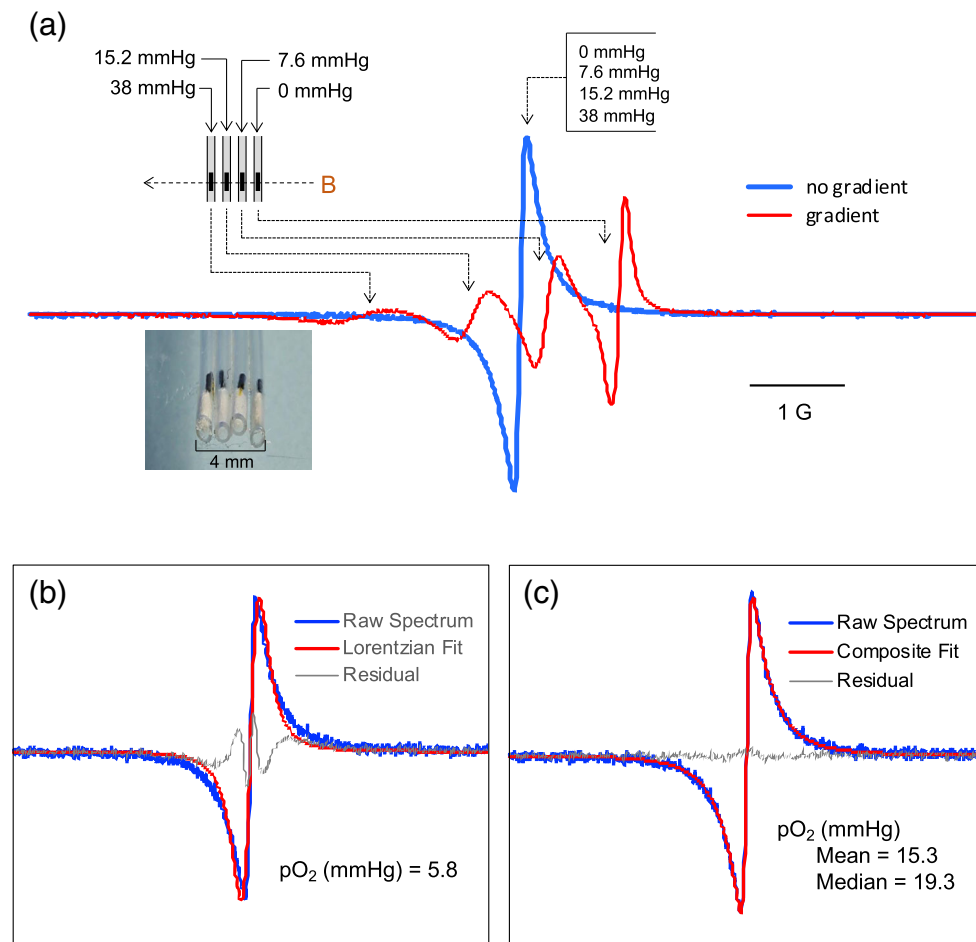


**Fig. 8** Oxygen measurement using multiple mChips. The utility of mChip for making simultaneous measurements of tissue  $pO_2$  using multiple chips was evaluated using a phantom containing 4 chips, each separately equilibrated with a gas mixture composed of different  $pO_2$ , namely 0, 7.6, 15.2 and 38.0 mmHg. L-band EPR measurements were performed in the presence/absence of a magnetic field gradient. **a** Phantom construction with 4 capillaries arranged in a flat/parallel configuration, each containing one mChip and connected to a gas perfusion line. Gas mixtures with different  $pO_2$  were flown through the chips at ambient pressure as indicated. A single EPR spectrum is seen in

the absence of magnetic field gradient. The presence of 4 chips are seen in the EPR spectrum obtained in the presence of a magnetic field gradient (6.5 G/cm across the plane of the tubes as shown in the inset). **b** A single Lorentzian fit to the spectrum obtained in the absence of magnetic field gradient shows a  $pO_2$  value of 5.8 mmHg, which is largely underestimated. **(c)** Composite fit to the spectrum obtained in the absence of magnetic field gradient reveals 15.3 mmHg and 19.3 mmHg as mean and median, respectively, which closely agree with the input values. The results indicate that multiple chips can be used to measure mean and median  $pO_2$  using a single scan without magnetic field gradient

in the form of mean and median values, which may be potentially useful for those tissues characterized with significant heterogeneity in oxygen distribution. The chip is biocompatible and stable in tissues without loss of EPR or oxygen sensitivity for extended periods of time. Preliminary evaluations in healthy and cancer tissues suggested that the sensor can provide repeated, robust, reliable and noninvasive monitoring of tissue oxygenation.

The mChips used in the muscle  $pO_2$  measurements were implanted at a depth of 2–4 mm from the skin. Post-surgical

removal of the mChips confirmed that they were in the superficial tissue, and in some cases the chips were found in the subcutaneous space. We think that the placement of the chips close to the subcutaneous space might be the reason for significantly lower  $pO_2$  values, for example 4–6 mmHg in some mice (Figs. 9d, 10e), compared to about 20 mmHg in the leg muscle of rats measured using OxyChip (Hou et al. 2018).

The smaller size of the mChip, compared to OxyChip, enables implantation of multiple sensors in the same tissue. In the past, signals from multiple implants were separated

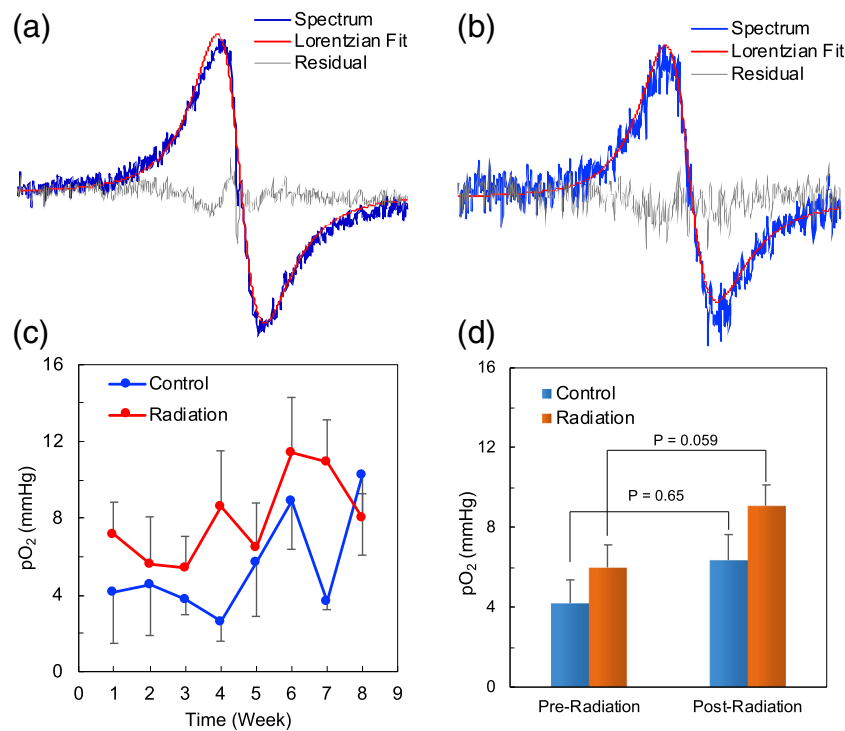


**Fig. 9** Repeated *in vivo* measurements of muscle pO<sub>2</sub> using a single mChip. The utility of mChip for making repeated *in vivo* measurements of muscle pO<sub>2</sub> was assessed in mice. A single implant of mChips was made in the biceps femoris of right limb of mice. pO<sub>2</sub> measurements were repeatedly made every week for 8 weeks in the muscle of control mice and mice muscle irradiated with a total of 36-Gy radiation, delivered in 2 × 6 Gy per week for the first 3 weeks. **a** Representative EPR spectra obtained from a control mouse (**a**) and an irradiated mouse (**b**) on week 4

are shown along with a single Lorentzian fit (and residuals). **c** Muscle pO<sub>2</sub> measured during the 8-week period from the control ( $N = 6$  mice) and irradiated muscle ( $N = 4$  mice). Data points represent Mean  $\pm$  SE. **d** Mean  $\pm$  SE values of muscle pO<sub>2</sub> during the first 3 weeks during irradiation (Pre-Radiation) and later 5 weeks (Post-Radiation) in comparison to unirradiated mice (Control). The results demonstrate the utility of mChip for making repeated *in vivo* measurements of tissue pO<sub>2</sub> over a period of weeks

using a magnetic field gradient, which posed certain restrictions and challenges including the requirement to keep the implants distributed in a particular configuration and maintain a minimum spacing between them (Grinberg et al. 2001; Khan et al. 2015; Smirnov et al. 1993). The current method using multiple mChips does not require prior knowledge of their number or geometrical distribution of them in the tissue and it uses a composite EPR signal measured without using a magnetic field gradient to obtain a pO<sub>2</sub> histogram (Ahmad et al. 2008). Although spatial information is not obtained by this procedure, the pO<sub>2</sub> histogram can be used to calculate mean and median pO<sub>2</sub> values, as commonly used in Eppendorf electrode methods (Vaupel et al. 2007).

Our results from the experimental phantom using multiple mChips clearly demonstrated the reliability of the composite spectral fitting approach. While the mChip-based composite spectral procedure provides better and more useful information regarding pO<sub>2</sub> distribution in a heterogeneous environment than a single implant, it does not substitute for a spatially-resolved imaging data (Elas et al. 2006; Epel and

Halpern 2015; Kuppasamy et al. 1998; Matsumoto et al. 2006, 2018), which may have far more information; however, at the expense of expensive hardware and data-acquisition time. The EPR measurements of mChips can be done in a matter of few seconds using the current scanners without any additional hardware requirements. Since the mChips are particularly developed for measuring oxygen in superficial tissues with implants at 1–4 mm depth, and further that they are compatible with pulsed mode EPR (Dayan et al. 2018; Wolfson et al. 2015, 2014; Zgazdai et al. 2018), the current bulky and complex CW EPR spectrometers can be replaced with simple, hand-held devices that are currently being developed and evaluated by our group for bedside or procedure-room clinical applications (Wolfson et al. 2015, 2014).

The mChip-based EPR oximetry will have potential applications as a biomarker in the following fields where repeated measurements of pO<sub>2</sub> in superficial tissues and tumors are considered important for treatment. For example, pO<sub>2</sub> measurements in cutaneous malignancies such as melanoma, basal cell carcinoma, and squamous cell carcinoma of the head and

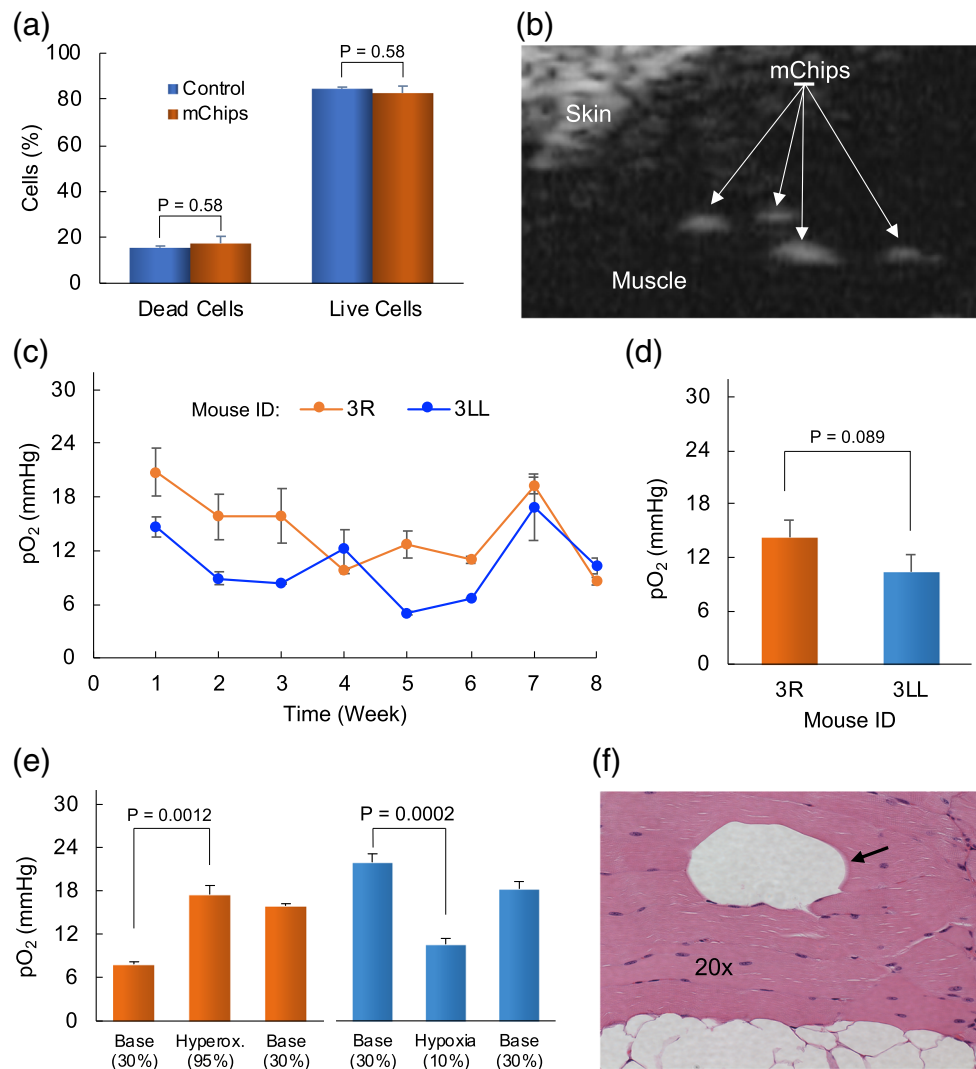


**Fig. 10** Repeated measurement of muscle pO<sub>2</sub> using multiple mChips. The effect mChips on the viability of muscle cells was determined by incubating L6 (muscle myoblast) cells for 48 h followed by Live/Dead cell staining. **a** The data show that there is no significant effect of mChips on cell viability. The feasibility of mChip for making repeated *in vivo* measurements of mean and median pO<sub>2</sub> using multiple chips was determined in mice muscle tissue. Four implants of mChips were made in biceps femoris of right limb of mice. pO<sub>2</sub> measurements were repeatedly made every week for 8 weeks. Panel **(b)** shows a representative ultrasound image revealing the presence of 4 mChips in the muscle. **c** Average values of muscle pO<sub>2</sub> (Mean ± SE; N = 5 measurements) computed from the composite spectra measured from 2 mice (ID: 3R and 3LL) for 8 weeks. **d** Average pO<sub>2</sub> values (Mean ± SE; N = 8 weeks) in each mouse over the 8-week period, showing no significant difference in

their pO<sub>2</sub> values. **e** pO<sub>2</sub> values (Mean ± SE; N = 5 measurements) obtained in two representative mice breathing sequentially (i) 30% oxygen (Base) for 20 min, carbogen (95% O<sub>2</sub> + 5% CO<sub>2</sub>) gas (Hyperox.) for 20 min and back to 30% oxygen (Base) for 20 min; or (ii) 30% oxygen (Base) for 20 min, 10% oxygen (Hypoxia) for 20 min and back to 30% oxygen (Base) for 20 min; **(f)** H&E-stained image of muscle tissue section (thickness, 5 μm) recovered after 8 weeks. The arrow points to the region where the chip was present. There is no indication of any foreign body inflammatory response or formation of fibrosis surrounding the chip. No leakages of LiNc-BuO crystals are found in the track and surrounding muscle. The results demonstrate the utility of mChip for making repeated *in vivo* measurements of mean pO<sub>2</sub> using multiple chips

neck (HN), cutaneous T cell lymphomas (CTCL), radiation-induced fibrosis of skin and underlying tissues exposed to ionizing radiation or subjected to surgical resection can be made noninvasively and repeatedly with mChip. Chemotherapy-induced peripheral neurotoxicity (CIPN) is

one of the least predictable and most prolonged sequelae with effects ranging from pain, numbness and tingling to diffuse weakness sometimes to the extent of paralysis. EPR oximetry with mChip can provide an early marker of disease onset. Tissue oxygen measurement has been identified as a critical

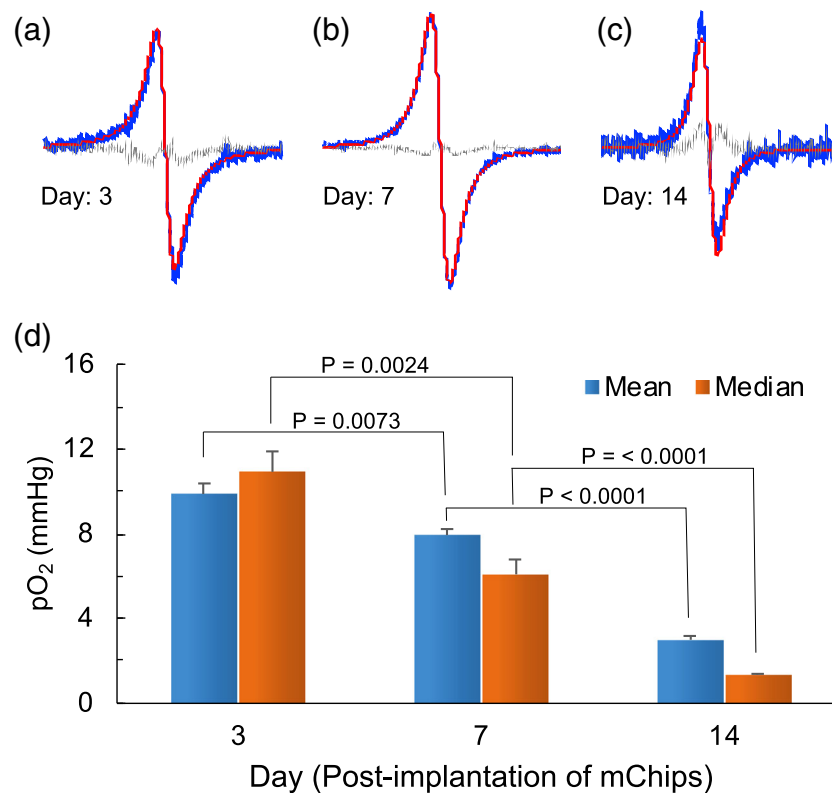


**Fig. 11** Repeated measurement of tumor pO<sub>2</sub> using multiple mChips. The utility of mChip for making repeated *in vivo* measurements of mean and median pO<sub>2</sub> was evaluated in a tumor model. Four implants of mChips were made in a human pancreatic cancer (AsPC-1) xenograft in mice. pO<sub>2</sub> measurements were repeatedly made during tumor growth. **a–c** Representative EPR spectra obtained from a tumor on day 3, 7 and 14

after implantation of the chips. **d** Mean and median representation of pO<sub>2</sub> values obtained on days 3, 7 and 14. Data represent Mean ± SE (N = 6 measurements) and Median ± SE (N = 6 measurements) with significance as noted. The results demonstrate the ability of mChip for making repeated *in vivo* measurements of mean and median pO<sub>2</sub> in tumors using multiple chips

step in diagnosing lower extremity chronic wounds, because it is a well-established, absolute predictor of wound healing potential and can help determine the correct therapy for treating a patient's wound. We are highly optimistic that EPR oximetry with mChip has the potential to fulfill the unmet clinical need.

## 5 Summary & conclusion

We have developed and validated the performance of a micro version of oxygen-sensing chip (mChip) for repeated measurement of oxygen concentration in superficial tissues. The microchips were stable against sterilization procedures or high energy radiation. The suitability and applicability of these novel oxygen sensors for long-term *in vivo* oximetry were determined by monitoring the oxygenation of murine muscle tissues and tumors. Overall, the study established the mChip as a promising choice of probe for clinical EPR oximetry. The microchip will enhance our ability to measure superficial tissue oxygenation with high sensitivity and reliability and

expand the applicability of the technology for a wide range of pre-clinical and clinical studies.

**Acknowledgements** This study was supported by National Institutes of Health (NIH) grant R01 EB004031. We acknowledge the support of P01 CA190193 for providing the motivation for development of the mChip for clinical studies. We thank Dr. Sassan Hodge for help with histopathology analysis and the clinician scientists, Drs. Philip E. Schaner, Eunice Y. Chen, and Victoria Lawson, for their overall enthusiasm for possible clinical potential of this technology.

## References

- R. Ahmad, P. Kuppasamy, Theory, instrumentation, and applications of electron paramagnetic resonance oximetry. *Chem. Rev.* **110**, 3212–3236 (2010)
- R. Ahmad, D.S. Vikram, L.C. Potter, P. Kuppasamy, Estimation of mean and median pO<sub>2</sub> values for a composite EPR spectrum. *J. Magn. Reson.* **192**, 269–274 (2008)
- N. Dayan, Y. Ishay, Y. Artzi, D. Cristea, E. Reijerse, P. Kuppasamy, A. Blank, Advanced surface resonators for electron spin resonance of single microcrystals. *Rev. Sci. Instrum.* **89**, 124707 (2018)

- M. Elas, K.H. Ahn, A. Parasca, E.D. Barth, D. Lee, C. Haney, H.J. Halpern, Electron paramagnetic resonance oxygen images correlate spatially and quantitatively with Oxylite oxygen measurements. *Clin. Cancer Res.* **12**, 4209–4217 (2006)
- B. Epel, H.J. Halpern, *In vivo* pO<sub>2</sub> imaging of tumors: Oxymetry with very low-frequency electron paramagnetic resonance. *Methods Enzymol.* **564**, 501–527 (2015)
- O.Y. Grinberg, A.I. Smimov, H.M. Swartz, High spatial resolution multi-site EPR oximetry. The use of convolution-based fitting method. *J. Magn. Reson.* **152**, 247–258 (2001)
- G. He, S.P. Evalappan, H. Hirata, Y. Deng, S. Petryakov, P. Kuppusamy, J.L. Zweier, Mapping of the B1 field distribution of a surface coil resonator using EPR imaging. *Magn. Reson. Med.* **48**, 1057–1062 (2002)
- H. Hou, N. Khan, S. Gohain, C.J. Eskey, K.L. Moodie, K.J. Maurer, H.M. Swartz, P. Kuppusamy, Dynamic EPR oximetry of changes in intracerebral oxygen tension during induced thromboembolism. *Cell Biochem. Biophys.* **75**, 285–294 (2017a)
- H. Hou, N. Khan, P. Kuppusamy, Measurement of pO<sub>2</sub> in a pre-clinical model of rabbit tumor using OxyChip, a paramagnetic oxygen sensor. *Adv. Exp. Med. Biol.* **977**, 313–318 (2017b)
- H. Hou, N. Khan, S. Gohain, M.L. Kuppusamy, P. Kuppusamy, Pre-clinical evaluation of OxyChip for long-term EPR oximetry. *Biomed. Microdevices* **20**, 29 (2018)
- G. Ilangovan, A. Bratasz, H. Li, P. Schmalbrock, J.L. Zweier, P. Kuppusamy, *In vivo* measurement and imaging of tumor oxygenation using coembedded paramagnetic particulates. *Magn. Reson. Med.* **52**, 650–657 (2004a)
- G. Ilangovan, T. Liebgott, V.K. Kutala, S. Petryakov, J.L. Zweier, P. Kuppusamy, EPR oximetry in the beating heart: Myocardial oxygen consumption rate as an index of posts ischemic recovery. *Magn. Reson. Med.* **51**, 835–842 (2004b)
- N. Khan, B.B. Williams, H. Hou, H. Li, H.M. Swartz, Repetitive tissue pO<sub>2</sub> measurements by electron paramagnetic resonance oximetry: Current status and future potential for experimental and clinical studies. *Antioxid. Redox Signal.* **9**, 1169–1182 (2007)
- N. Khan, H. Hou, C.J. Eskey, K. Moodie, S. Gohain, G. Du, S. Hodge, W.C. Culp, P. Kuppusamy, H.M. Swartz, Deep-tissue oxygen monitoring in the brain of rabbits for stroke research. *Stroke* **46**, e62–e66 (2015)
- M.M. Kmiec, H. Hou, M.L. Kuppusamy, T.M. Drews, A.M. Prabhat, S.V. Petryakov, E. Demidenko, P.E. Schaner, J.C. Buckley, A. Blank, et al., Application of SPOT chip for transcutaneous oximetry. *Magn. Reson. Med.* **81**, 2837–2840 (2019)
- M.C. Krishna, S. English, K. Yamada, J. Yoo, R. Murugesan, N. Devasahayam, J.A. Cook, K. Golman, J.H. Ardenkjaer-Larsen, S. Subramanian, et al., Overhauser enhanced magnetic resonance imaging for tumor oximetry: Coregistration of tumor anatomy and tissue oxygen concentration. *Proc. Natl. Acad. Sci. U. S. A.* **99**, 2216–2221 (2002)
- A.C. Kulkarni, P. Kuppusamy, N. Parinandi, Oxygen, the lead actor in the pathophysiological drama: Enactment of the trinity of normoxia, hypoxia, and hyperoxia in disease and therapy. *Antioxid. Redox Signal.* **9**, 1717–1730 (2007)
- P. Kuppusamy, M. Afeworki, R.A. Shankar, D. Coffin, M.C. Krishna, S.M. Hahn, J.B. Mitchell, J.L. Zweier, *In vivo* electron paramagnetic resonance imaging of tumor heterogeneity and oxygenation in a murine model. *Cancer Res.* **58**, 1562–1568 (1998)
- Kuppusamy, P., Kmiec, M.M., Dan, T., Mast, J.M., and Ahmad, R. (2019). Estimation of pO<sub>2</sub> histogram from a composite EPR spectrum of discrete random implants. To be published
- J.M. Mast, P. Kuppusamy, Hyperoxygenation as a therapeutic supplement for treatment of triple negative breast Cancer. *Front. Oncol.* **8**, 527 (2018)
- K. Matsumoto, S. Subramanian, N. Devasahayam, T. Aravalluvan, R. Murugesan, J.A. Cook, J.B. Mitchell, M.C. Krishna, Electron paramagnetic resonance imaging of tumor hypoxia: Enhanced spatial and temporal resolution for *in vivo* pO<sub>2</sub> determination. *Magn. Reson. Med.* **55**, 1157–1163 (2006)
- K.I. Matsumoto, S. Kishimoto, N. Devasahayam, G.V.R. Chandramouli, Y. Ogawa, S. Matsumoto, M.C. Krishna, S. Subramanian, EPR-based oximetric imaging: A combination of single point-based spatial encoding and T1 weighting. *Magn. Reson. Med.* **80**, 2275–2287 (2018)
- G. Meenakshisundaram, E. Eteshola, R.P. Pandian, A. Bratasz, S.C. Lee, P. Kuppusamy, Fabrication and physical evaluation of a polymer-encapsulated paramagnetic probe for biomedical oximetry. *Biomed. Microdevices* **11**, 773–782 (2009a)
- G. Meenakshisundaram, E. Eteshola, R.P. Pandian, A. Bratasz, K. Selvendiran, S.C. Lee, M.C. Krishna, H.M. Swartz, P. Kuppusamy, Oxygen sensitivity and biocompatibility of an implantable paramagnetic probe for repeated measurements of tissue oxygenation. *Biomed. Microdevices* **11**, 817–826 (2009b)
- A.T. Mobashsher, A.M. Abbosh, Artificial human phantoms: Human proxy in testing microwave apparatuses that have electromagnetic interaction with the human body. *IEEE Microw. Mag.* **16**, 42–62 (2015)
- I.K. Mohan, M. Khan, S. Wisel, K. Selvendiran, A. Sridhar, C.A. Carnes, B. Bogner, T. Kalai, K. Hideg, P. Kuppusamy, Cardioprotection by HO-4038, a novel verapamil derivative, targeted against ischemia and reperfusion-mediated acute myocardial infarction. *Am. J. Physiol. Heart Circ. Physiol.* **296**, H140–H151 (2009)
- R.P. Pandian, N.L. Parinandi, G. Ilangovan, J.L. Zweier, P. Kuppusamy, Novel particulate spin probe for targeted determination of oxygen in cells and tissues. *Free Radic. Biol. Med.* **35**, 1138–1148 (2003)
- J.D. Pollock, B.B. Williams, J.W. Sidabras, O. Grinberg, I. Salikhov, P. Lesniewski, M. Kmiec, H.M. Swartz, Surface loop resonator design for *in vivo* EPR tooth dosimetry using finite element analysis. *Health Phys.* **98**, 339–344 (2010)
- I. Salikhov, H. Hirata, T. Walczak, H.M. Swartz, An improved external loop resonator for *in vivo* L-band EPR spectroscopy. *J. Magn. Reson.* **164**, 54–59 (2003)
- A.I. Smimov, S.W. Norby, R.B. Clarkson, T. Walczak, H.M. Swartz, Simultaneous multi-site EPR spectroscopy *in vivo*. *Magn. Reson. Med.* **30**, 213–220 (1993)
- H.M. Swartz, H. Hou, N. Khan, L.A. Jarvis, E.Y. Chen, B.B. Williams, P. Kuppusamy, Advances in probes and methods for clinical EPR oximetry. *Adv. Exp. Med. Biol.* **812**, 73–79 (2014a)
- H.M. Swartz, B.B. Williams, B.I. Zaki, A.C. Hartford, L.A. Jarvis, E.Y. Chen, R.J. Comi, M.S. Ernstoff, H. Hou, N. Khan, et al., Clinical EPR: unique opportunities and some challenges. *Acad. Radiol.* **21**, 197–206 (2014b)
- P. Vaupel, M. Hockel, A. Mayer, Detection and characterization of tumor hypoxia using pO<sub>2</sub> histography. *Antioxid. Redox Signal.* **9**, 1221–1235 (2007)
- S.S. Velan, R.G. Spencer, J.L. Zweier, P. Kuppusamy, Electron paramagnetic resonance oxygen mapping (EPROM): Direct visualization of oxygen concentration in tissue. *Magn. Reson. Med.* **43**, 804–809 (2000)

- H. Wolfson, R. Ahmad, Y. Twig, P. Kuppusamy, A. Blank, A miniature electron spin resonance probehead for transcutaneous oxygen monitoring. *Appl. Magn. Reson.* **45**, 955–967 (2014)
- Wolfson, H., Ahmad, R., Twig, Y., Blank, A., and Kuppusamy, P. (2015). A hand-held EPR scanner for transcutaneous oximetry. *Proc. SPIE 9417, Medical Imaging 2015: Biomedical Applications in Molecular, Structural, and Functional Imaging*
- O. Zgadzi, Y. Twig, H. Wolfson, R. Ahmad, P. Kuppusamy, A. Blank, Electron-spin-resonance dipstick. *Anal. Chem.* **90**, 7830–7836 (2018)

**Publisher's note** Springer Nature remains neutral with regard to jurisdictional claims in published maps and institutional affiliations.